Neuropsychologia 135 (2019) 107236

Contents lists available at ScienceDirect

Neuropsychologia

journal homepage: http://www.elsevier.com/locate/neuropsychologia

The oblique effect: The relationship between profiles of visuospatial preference, cognition, and brain connectomics in older adults

Jamie C. Peven [a,b], Yurong Chen [c], Lei Guo [c], Liang Zhan [c], Elizabeth A. Boots [d,e], Catherine Dion [f], David J. Libon [g,h], Kenneth M. Heilman [i], Melissa Lamar [e,j,*]

[a] *Department of Psychology, University of Pittsburgh, Pittsburgh, PA, United States*
[b] *Center for the Neural Basis of Cognition, University of Pittsburgh, Pittsburgh, PA, United States*
[c] *Department of Electrical and Computer Engineering, University of Pittsburgh, Pittsburgh, PA, USA*
[d] *Department of Psychology, University of Illinois at Chicago, Chicago, IL, USA*
[e] *Rush Alzheimer's Disease Center, Rush University Medical Center, Chicago, IL, USA*
[f] *Department of Clinical and Health Psychology, University of Florida, Gainesville, FL, USA*
[g] *Department of Geriatrics and Gerontology, New Jersey Institute for Successful Aging, School of Osteopathic Medicine, Rowan University, USA*
[h] *Department of Psychology, New Jersey Institute for Successful Aging, School of Osteopathic Medicine, Rowan University, USA*
[i] *Department of Neurology, University of Florida College of Medicine, Gainesville, FL, USA*
[j] *Department of Psychiatry and Behavioral Sciences, Rush University Medical Center, Chicago, IL, USA*

ARTICLE INFO

Keywords:
Aging
Perception
Executive function
Oblique effect
Structural connectivity
Visuospatial processing

ABSTRACT

The *oblique effect* (OE) describes the visuospatial advantage for identifying stimuli oriented horizontally or vertically rather than diagonally; little is known about brain aging and the OE. We investigated this relationship using the Judgment of Line Orientation (JLO) in 107 older adults (~age = 67.8 ± 6.6; 51% female) together with neuropsychological tests of executive functioning (EF), attention/information processing (AIP), and neuroimaging. Only JLO lines falling between 36-54° or 126–144° were considered oblique. To quantify the oblique effect, we calculated z-scores for oblique errors (zOblique = #oblique errors/#oblique lines), and similarly, horizontal + vertical line errors (zHV), and a composite measure of oblique relative to HV errors (zOE). Composite z-scores of EF and AIP reflected domains associated with JLO performance. Graph theory analysis integrated T1-derived volumetry and diffusion MRI-derived white matter tractography into connectivity matrices analyzed for select network properties. Participants produced more zOblique than zHV errors ($p < 0.001$). Age was not associated with zOE adjusting for sex, education, and MMSE. Similarly adjusted linear regression models revealed that lower EF was associated with a larger oblique effect ($p < 0.001$). Modular analyses of neural connectivity revealed a differential patterns of network affiliation that varied by high versus low group status determined via median split of zOblique and zHV errors, separately. Older adults exhibit the oblique effect and it is associated with specific cognitive processes and regional brain networks that may facilitate future investigations of visuospatial preference in aging.

1. Introduction

The *oblique effect* represents a "consistent superiority in performance when visual stimuli are horizontal or vertical, as opposed to oblique" or on a diagonal (Appelle, 1972). Ophthalmological, neurophysiological, and psychological literature suggest that the oblique effect is consistently observed in humans (Arakawa et al., 2000; Attneave and Olson, 1967; Essock, 1980; Higgins and Stultz, 1950; Maffei and Campbell, 1970; McMahon and Macleod, 2003; Orban et al., 1984; Westheimer, 2003) and multiple animal species (De Valois, Yund and Hepler, 1982; Geisler and Albrecht, 1997; Li et al., 2003), including non-human primates (De Valois et al., 1982; Mansfield, 1974). The oblique effect has been noted as early as three months of age in humans (Leehey et al., 1975; Sokol et al., 1987), suggesting this phenomenon is innate, rather than learned. Despite the many changes in brain structure and cognition that occur with age, less is known about how aging and age-related cognitive profiles are associated with the oblique effect.

To our knowledge, only two studies have examined the oblique effect

---

* Corresponding author. Rush Alzheimer's Disease Center, Rush University Medical Center, 1750 W. Harrison Street, Suite 1000, Chicago, IL 60612, USA.
E-mail addresses: jac349@pitt.edu (J.C. Peven), melissa_lamar@rush.edu (M. Lamar).

https://doi.org/10.1016/j.neuropsychologia.2019.107236
Received 13 May 2019; Received in revised form 20 September 2019; Accepted 18 October 2019

in older adults and only one of which reported results specific to normal cognitive aging. While mid-to late-life healthy control participants tended to mis-identify one oblique line for another, the oblique effect, defined as greater errors during oblique *relative to* non-oblique (i.e., horizontal or vertical) line identification, was not explicitly investigated (Ska et al., 1990). Meanwhile, participants with dementia made more oblique line and non-oblique line errors indiscriminately when compared to controls (Ska et al., 1990) suggesting that patients with probable Alzheimer's dementia showed visuospatial impairment characteristic of global judgment errors on line orientation. Finton and colleagues (Finton et al., 1998) further confirmed that when compared to healthy controls, participants with Alzheimer's dementia failed to display any specific error phenotype. Some researchers hypothesize that subtle cognitive alterations in visuospatial functions may be an early indicator for the development of dementia (Cabeza et al., 2004; Dolcos et al., 2002; Lamar et al., 2016), as opposed to emerging as a global phenotype seen at later stages of disease (Finton et al., 1998; Ska et al., 1990). Thus, investigating for the presence of the oblique effect and how this error profile is potentially altered by age, and age-associated cognition and/or brain structure, may help to identify early cognitive markers of neurodegenerative disease in vulnerable individuals.

In the past two decades, neurophysiological and neuroimaging research on the oblique effect has provided converging evidence of distinct regional brain involvement in the divergent line orientations that contribute to this form of visuospatial advantage. For example, animal studies investigating the oblique effect report that neurons in the striate cortex respond more frequently to horizontal and vertical stimuli than oblique stimuli (Bonds, 1982; Coppola et al., 1998; De Valois et al., 1982; Dragoi et al., 2000; Li et al., 2003). Furthermore, studies of visual evoked response potentials in humans demonstrate a more robust response in the striate cortex to horizontal and vertical stimuli than they do to oblique stimuli (Arakawa et al., 2000; Maffei and Campbell, 1970; Sokol et al., 1987). Neuroimaging results using functional magnetic resonance imaging (fMRI) also report increased blood oxygenation level dependent (BOLD) responses within the striate cortex during the presentation of horizontal and vertical task items compared to oblique-oriented items (Furmanski and Engel, 2000). Little work exists attempting to extend these results – specifically, higher striate involvement when viewing horizontal and vertical versus oblique-oriented lines – to feedforward connections, i.e., extrastriate areas or other cortical regions, particularly as it relates to oblique effect error profiles in humans. The research that does exist comes from lesion studies of overall performance on judgments of line orientation suggesting right (greater than left) posterior involvement (Benton et al., 1975; Mehta and Newcome, 1991). Recent advances in neuroimaging may provide an in-depth opportunity to examine the organizational networks that mediate the oblique effect in healthy older adults.

Connectomics allows for a graph-theoretical assessment of system properties in order to understand quantitatively how brain regions, or 'nodes', communicate and interact (Rubinov and Sporns, 2010). Additionally, advanced graph-theoretical 'modularity analysis' investigates how a group of nodes preferentially interact among themselves to form a community or module, which can then be compared between groups of brain networks to assess for 'modular' differences (GadElkarim et al., 2012; Ye et al., 2015). Understanding the age-related associates of oblique effect error profiles, as well as the brain connectome neurocircuitry underpinning it, may enhance our knowledge of this long-studied visuospatial phenomenon of in older adults given the paucity of work conducted in older adults to date (Finton et al., 1998; Ska et al., 1990), and foster future work investigating subtle visuospatial markers of pathological aging.

The present study focused on the relationships between aging, cognition, neural connectivity, and the oblique effect in 107 non-demented, non-depressed older adults. We first hypothesized that 1a) older adults would make more errors on oblique lines compared to horizontal and vertical (HV) lines after controlling for relevant confounders; and, 1b) age would be positively associated with the oblique effect after controlling for relevant confounders. Previous research has documented the importance of executive functioning and, to a lesser degree, attention/information processing to the alterations seen in visuospatial processing in older adults regardless of dementia (Freeman et al., 2000; Lamar et al., 1997). Thus, our second hypothesis was that lower performance on an executive function composite would be associated with a larger oblique effect, i.e., a higher number of oblique relative to HV errors, after controlling for relevant confounders. Given that older age and lower performance on executive function tasks have both been associated with reductions in white matter integrity and altered structural connectivity in otherwise healthy older adults (Charlton et al., 2006; Charlton et al., 2010; Gonzales et al., 2017; Lamar et al., 2016), our third and final hypothesis was that a larger oblique effect would be associated with lower graph-theoretical metrics of neural connectivity and that higher levels of oblique errors but not HV errors would be associated with distinct modularity within anterior (i.e., prefrontal) regions of brain.

2. Materials and methods

2.1. Participants

Individuals aged 60 or older from three self-reported ethnic/racial categories (i.e., African American, non-Latinx white, and Latinx) were recruited via community outreach (e.g., advertisements and fliers), word of mouth, and research registries to participate in a study of healthy aging and cardiovascular disease risk factors at the University of Illinois at Chicago (UIC) Department of Psychiatry. The study was approved by the UIC Institutional Review Board (IRB) as well as the Rush University Medical Center IRB and conducted in accordance with the Declaration of Helsinki with written informed consent obtained from all participants.

An initial telephone screen conducted in participants' language of choice (English or Spanish) determined preliminary study eligibility. Based on this screen, potential participants were excluded if there was any self-reported current or past history of neurological conditions including Alzheimer's disease or any other form of dementia or mild cognitive impairment, Parkinson's disease, stroke, or seizures, current or past history of Axis I or Axis II psychiatric disorders (e.g., depression, bipolar disorder), a history of head injury or loss of consciousness, a present or past history of substance abuse or dependence, psychotropic medication use, or contraindications for magnetic resonance imaging (MRI). A history of stable (e.g., diabetes) or remitted medical illness (e.g., cancer) was not an exclusionary factor.

Following the initial telephone screen, participants were scheduled for a more detailed evaluation in their language of choice, including cognitive (i.e., Mini-Mental State Examination; MMSE) (Folstein et al., 1975) and affective (i.e., Structured Clinical Interview for DSM-IV; SCID) (Spitzer et al., 1992) screens for final inclusion or exclusion determination. All screening measures were administered by a trained research assistant fluent in either English or Spanish and these screenings were followed by an evaluation by a board eligible psychiatrist who completed the 17-item Hamilton Depression Rating Scale (HAM-D) (Hamilton, 1960). All raters were blind to telephone screen information.

Final inclusion criteria consisted of an absence of psychiatric symptoms based on the SCID and a score $\leq$8 on the HAM-D, as well as an MMSE $\geq$24. All study participants completed the Beck Depression Inventory (BDI) (Beck et al., 1996) and the Beck Anxiety Inventory (BAI) (Beck and Steer, 1990) for subjective measurements of depressive and anxiety symptomatology, respectively. In total, 121 participants were deemed eligible for inclusion based on the above criteria.

Of these 121 individuals who met eligibility criteria, 9 were excluded from the current project for either missing JLO data ($n = 2$) or neuroimaging ($n = 7$). An additional 5 participants were excluded secondary to scanner problems ($n = 2$) or incidental findings ($n = 3$). A total of 107 participants were included in the final sample for the neuroimaging portion of this study. A total of 97 individuals received their neuropsychological evaluation in English; only this subset of participants was used for analyses involving cognitive composite scores.

2.2. Study protocol

2.2.1. Judgment of Line Orientation Test

To test the oblique effect in our sample, we employed the Judgment of Line Orientation Test (JLO) Form H (Benton et al., 1983), a test requiring both visuospatial and executive functions to complete successfully. Standardized administration and scoring were implemented in participants' preferred language (equivalency has been documented for JLO performance in English and Spanish; Rey, Feldman, Rivas-Vazquez, Levin and Benton, 1999). When being tested with the JLO, participants are shown an array of 11 key lines angled to create a semicircle (Fig. 1). These key lines, numbered 1–11, remain in the participant's view as a reference for the duration of the task. During a brief practice session to prepare participants for the test, they are shown two lines identical in length to the key-reference lines and are asked to report the corresponding numbers of the key lines that match the practice items. Feedback is provided across all 5 practice trials; the JLO is discontinued if a participant does not improve and/or demonstrate understanding of the task. The JLO consists of 30 consecutive trials, each with two test lines presented simultaneously that are shorter than the key-reference lines. Participants earn one point for each trial in which both test lines are correctly identified and zero points if one or both lines are incorrectly identified (maximum total score = 30). Unlike the practice session, no feedback about the participant's performance is provided during the test session.

To quantify the oblique effect error profile (i.e., greater oblique versus HV errors), we identified the key lines within the semi-circle reference array that were close to the 45-degree angle (i.e., lines 3, 4, 8, & 9 fell within a 36-54° or a 126–144° range) and within the degree range delineated by prior research (e.g., 30–60°; Appelle, 1972), and labeled them 'oblique' (total oblique lines presented across all JLO test trials = 19). Given the precedent set in prior literature of using only horizontal and vertical lines as 'non-oblique' (Appelle, 1972), only horizontal (i.e., 1 & 11) and vertical (i.e., 6) lines were included for analytic comparisons against oblique lines (total horizontal + vertical lines presented across all JLO test trials = 16). The remaining four lines in the JLO array were not horizontal or vertical and also fell outside the oblique line angle range (i.e., lines 2, 5, 7, & 10 were positioned at 18, 72, 108, or 162°, respectively); thus, they were not included in our analysis of the oblique effect, but they did contribute to overall JLO scores.

Using the inverse of the JLO standardized scoring system, we noted the number of test lines from all 30 trial line pairs participant *incorrectly* identified (i.e., 0, 1, or 2 per trial; maximum score = 60). We then tallied errors that corresponded to 'oblique' lines (maximum errors possible = 19) and errors that corresponded to horizontal and vertical lines (maximum errors possible = 16). Given the unequal number of oblique lines to horizontal and vertical lines, and to compare appropriately within subjects for the oblique effect, scores were calculated, then z-transformed prior to consolidation into the composite metric outlined below:

Oblique Line Errors (zOblique) = Total number of incorrect oblique lines/Total number of possible oblique line responses.

Horizontal and Vertical Line Errors (zHV) = (Total number of incorrect horizontal lines + Total number of incorrect vertical lines)/ Total number of possible horizontal and vertical line responses.

Oblique Effect (zOE) = zOblique/zHV. In order to create a single metric that represented poor perception of oblique lines relative to non-oblique lines, we created a composite score using zOblique and zHV scores as indicated by the equation above. We then multiplied the resulting quotients by −1 so that a higher z-score signaled a larger oblique effect, i.e., more errors on oblique lines relative to HV lines.

2.2.2. Neuropsychological assessment

A comprehensive neuropsychological assessment conducted by trained research assistants included standardized measures of episodic memory, language, attention, executive and visuospatial functioning. For the current study, composite z-scores were created based on averaging individual z-scores taken from tests of executive functioning (EF) and attention/information processing (AIP). These scores were reversed where appropriate so that higher scores reflected better performance.

The EF composite score consisted of time (in seconds) for completion of the Trail Making Test (TMT) Part B (Reitan and Wolfson, 1985), the Wechsler Abbreviated Scale of Intelligence - II Matrix Reasoning raw score (Wechsler, 1997), and a measure of graphomotor planning from the digital Clock Drawing Test, i.e., the presence or absence of initial digit placement as the 12, 3, 6, and 9, or 'anchoring,' during task completion that has been shown to associate with executive functioning and structural connectivity with the prefrontal cortex (Lamar et al., 2016). The AIP composite score consisted of time to completion in seconds for both the TMT Part A and Part 'M' motor analogue consisting of empty circles connected with a visible dotted line that participants were asked to follow for a measure of motor speed, as well as the Wechsler Adult Intelligence Scale - IV Coding raw score (Wechsler, 2014). These domains were based on theoretical groupings of similar test variables of interest (Charlton et al., 2014; Cohen et al., 2014; Lamar et al., 2015). Cronbach's alphas provided a metric of how well each score measured a unidimensional latent construct: EF $\alpha = 0.57$ and AIP $\alpha = .64$.

2.3. Neuroimaging protocol

2.3.1. Data acquisition

Whole brain MRI was acquired on a GE 3.0T whole body scanner (MR 750 Discovery, General Electric Health Care, Waukesha, Wisconsin)

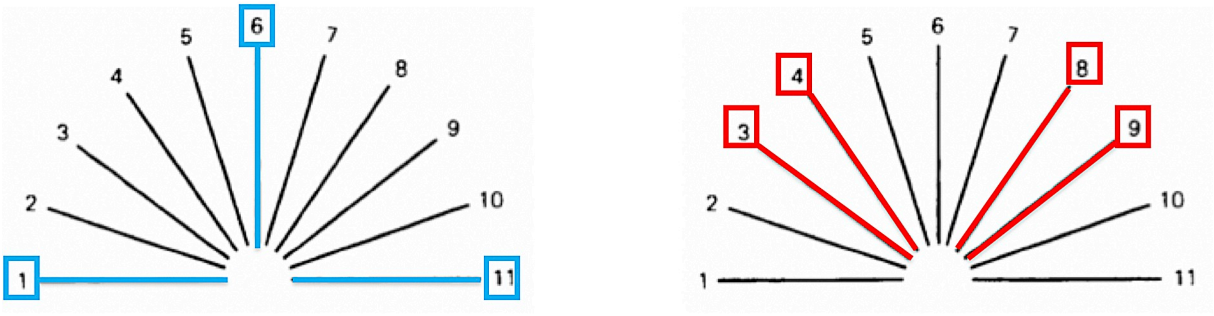

Fig. 1. A modified JLO array that shows horizontal/vertical lines (left, blue) and oblique lines (right, red). (For interpretation of the references to colour in this figure legend, the reader is referred to the Web version of this article.)

using an 8-channel head coil. Participants were positioned comfortably on the scanner bed and fitted with soft ear plugs; foam pads were used to minimize head movement. Participants were instructed to remain still throughout the scan. DTI was acquired using 2-D spin-echo EPI sequence (FOV = 20 mm; voxel size = 0.78 × 0.78 × 3.0 mm; TR/TE = 5525/93.5 ms; flip angle = 90°). Forty interleaved axial slices aligned to the AC-PC line were collected in 32 gradient directions with b = 1400 s/mm^2 and 6 b_0 images. High resolution three-dimensional T_1-weighted images were acquired using a Brain Volume (BRAVO) image sequence (field of view: FOV = 22 mm^2; 120 interleaved axial slices 1.5 mm thick; TR/TE = 1200 ms/5.3 ms; flip angle = 13°; voxel size = 0.42 × 0.42 × 1.5 mm). These sequences were acquired as part of a larger neuroimaging protocol.

2.3.2. Image analysis

To generate connectome data and network efficiency information using graph theory analyses, a pipeline was constructed that integrates multiple image analysis techniques. Diffusion MRI was realigned to the b_0 image using the automatic image registration (AIR) algorithm with affine transformation to minimize eddy current distortions. This was followed by the computation of diffusion tensors and then deterministic tractography using Fiber Assignment by Continuous Tracking (FACT) algorithm built into the DTI-Studio program (Mori et al., 1999). For each subject, tractography was first performed by tracking the whole brain, initiating tracts at each voxel. Fiber tracking was stopped when the fractional anisotropy (FA) value fell below 0.15 or a turning angle became larger than 60°.

T_1-weighted images were used to generate label maps using FreeSurfer 6.0 (http://surfer.nmr.mgh.harvard.edu/) for volumetric segmentation (Desikan et al., 2006; Destrieux et al., 2010; Fischl et al., 2004). Each label map is composed of 82 different gray matter regions of interest (ROIs), which include cortical and subcortical regions, brainstem, and cerebellum.

In brief, we generated brain structural networks by counting the number of reconstructed streamlines resulting from diffusion MRI-derived whole brain white matter tractography described above that connected every pair of ROIs defined by FreeSurfer's parcellation atlas (i.e., the 82 ROIs); this in-house-developed pipeline has been previously published and described in greater detail in (Ajilore et al., 2014; Charlton et al., 2014; Lamar et al., 2016). The resulting matrices were then analyzed using the Brain Connectivity Toolbox (BCT) (Rubinov and Sporns, 2010). In order to minimize multiple comparisons of graph theory metrics, variables of interest were carefully selected to represent global and local system properties that have been shown to be associated with aging and cognitive function (Ajilore et al., 2014; Brown et al., 2011; Geerligs et al., 2015; Wen et al., 2011).

In graph theory, a network is a set of 'nodes' or brain regions with 'edges' or connections between them. It has been suggested that an optimized network can be described as exhibiting a balance between global integration (measured using network efficiency or shortest path length) and local segregation (measured using clustering coefficient) (Rubinov and Sporns, 2010, 2011). Our graph theory metrics of network system properties included measures of: 1) normalized clustering coefficient or Gamma, which quantifies the strength of interconnection among neighborhood nodes (higher clustering indicates that the immediate neighbors of a node tend to be immediate neighbors among themselves, thus collectively forming a tightly-knit "cluster"); 2) normalized characteristic path length or Lambda, which measures the averaged graph distance between nodes, thus indicating the overall efficiency in information transfer (lower path length represents higher efficiency); and 3) regional connectivity of a node (Wen et al., 2011), measured using the local efficiency, mathematically defined as global efficiency, i.e., how efficiently the entire network exchanges information, computed on neighborhood nodes (Rubinov and Sporns, 2010). Both 1 and 2 were normalized against 1000 randomly generated networks with the same number of nodes and edge distribution. These metrics were calculated using the Brain Connectivity Toolbox. For detailed description of the equations, please refer to (Rubinov and Sporns, 2010). Connectome data was visualized using BrainNet Viewer (Xia et al., 2013).

For connectome hierarchical modularity analysis, i.e., how local nodes or brain regions interact to form communities or modules, we employed the *path length associated community estimation* (PLACE) technique (GadElkarim et al., 2012, 2014), which was developed to compare a connectome's hierarchical modularity between groups. Instead of a well-known modularity metric that only considers the connections or edges at the intra-community level, PLACE extracts communities via optimal edge partition into two categories: connections *between* versus connections *within* communities. Previous work has shown this approach to be advantageous when compared to modularity metric Q (GadElkarim et al., 2014), namely PLACE does not suffer from the same resolution limits as Q. Mathematically, PLACE utilizes a path length-based novel metric and exploits powers of 2 to compute regularly hierarchical trees. In order to extract community structures at each tree-level using PLACE, nodes were assigned to one of two communities by maximizing the difference between the mean inter-modular and the mean intra-modular path lengths (GadElkarim et al., 2012, 2014). To quantify modular or community affiliation differences, PLACE, designed for various computational strategies, compared the scaled inclusivity metric "V" that quantifies affiliation 'mis-match' between two modular structures at a specific node or a specific community (V ranges from 0 to 1; 0 indicates no modular pattern is shared at this node while 1 indicates a complete match).

2.4. Confounders of the effect

Given the documented sex-differences in visuospatial functioning (Herlitz et al., 1999; Lewin et al., 2001), as well as brain morphometry (Cosgrove et al., 2007; Tunc et al., 2016) including white matter integrity (Kanaan et al., 2012), and the influence of education and associated general cognitive functioning on these same factors (Coffey et al., 1999; Ganguli et al., 2010), sex, education, and MMSE were considered as covariates. To confirm this decision, we performed unadjusted bivariate correlations as outlined below.

2.5. Statistical analyses

All analyses involving participant characteristics, cognitive variables, and the oblique effect error profiles were conducted using IBM SPSS Statistics 24. To confirm our decision regarding covariates for hypothesis testing, we performed unadjusted independent samples t-tests or bivariate correlations (as relevant) of sex, education, and MMSE performance as they related to zOblique and zHV errors, separately. To test our first hypotheses regarding the presence of the oblique effect and its association with age, a repeated measures general linear model adjusting for sex, education, and MMSE directly compared zOblique to zHV errors and two-tailed partial Pearson's product moment correlations investigated the relationship between age and zOE adjusted for sex, education, and MMSE. Separate ordinary least squares hierarchical linear regression analyses determined the relationship of cognitive domain composite z-scores of EF and AIP (separately) and our composite metric of the oblique effect (zOE) adjusting for sex, education, and MMSE.

Analyses of the relationships between the oblique effect as measured using zOE and our three connectome metrics were analyzed using separate ordinary least squares hierarchical linear regression analyses adjusting for sex, education, and MMSE. PLACE analysis used a median split to determine participants with relatively low levels of zOblique errors or relatively low levels of zHV errors as separate reference groups in order to test for high versus low group modular differences in the scaled inclusivity metric 'V' for zOblique and zHV error profiles (separately) using two-sample T-test adjusting for sex, education, and MMSE, with false discovery rate (FDR) correction for multiple comparisons. We chose to look at zOblique and zHV separately given that this was the method often used in previous neuroimaging research.

3. Results

3.1. Participants

When considering the full neuroimaging sample (N = 107), participants averaged 67 years of age and approximately 15 years of education (see Table 1 for details). The sample was almost half male (48.59%), with the majority of individuals self-identifying as either Latinx or Black (59.81%). As seen in Table 1, there were no differences between the neuroimaging sample and the cognitive subsample (n = 97) in terms of participant characteristics (all p-values ≥ 0.180).

Women showed a larger oblique effect as measured with zOE than men, t(105) = - 2.52, p = 0.014). Both lower education and lower MMSE scores were associated with a larger oblique effect (r(107) = -0.22, p = 0.022; r(107) = -0.19, p = 0.050, respectively). These results confirmed our a priori decision to include sex, education, and MMSE as covariates in hypothesis testing.

3.2. Judgment of Line Orientation

3.2.1. Overall JLO performance

All participants successfully completed the practice items at the outset of the JLO task. On average, participants correctly identified 22 out of 30 items on the JLO test trials (M = 21.89, SD = 4.90) (Table 2).

3.3. Aging, cognition, and the oblique effect

3.3.1. The oblique effect and its association with aging

Participants made more oblique errors when directly compared to HV errors, F(102) = 12.80, p = 0.001, after adjusting for sex, education, and MMSE. zOE, our composite index of oblique errors relative to HV errors, was not associated with age after adjusting for sex, education, and MMSE (r(102) = -0.90, p = 0.364).

3.3.2. Cognitive domains and the oblique effect

To investigate whether EF and AIP were associated with zOE, we conducted separate linear regression models adjusting for sex, education, and MMSE. Consistent with our prediction, lower EF was significantly associated with a larger oblique effect, β = −.46, t(87) = -3.97, p < 0.001 (Table 3). Adding a sex-by-EF interaction term to the significant zOE model did not result in a significant interaction; further, it did not alter the main effects reported above. AIP was not significantly associated with zOE (p = 0.191) in fully-adjusted regression models; therefore, a sex-by-AIP interaction term was not conducted.

Table 1
Participant characteristics.

	FULL SAMPLE (N = 107)	COGNITIVE SUB-SAMPLE (N = 97)	P
AGE	67.82 (6.69)	67.95 (6.71)	.893
SEX (M : F)	52 : 55	46 : 51	.868
% RIGHT-HANDED	90 (0.30)	90 (0.30)	.970
RACE (B : L : NLW)	46 : 18 : 43	46 : 8 : 43	.846
EDUCATION	15.55 (3.37)	16.14 (2.79)	.180
MMSE	28.72 (1.39)	28.73 (1.40)	.950
HAM-D	1.28 (1.65)	1.17 (1.50)	.643

NOTE: Values presented as mean (standard deviation) unless otherwise noted. Sex: M = male, F = female; % = percent; Race: B=Black, L = Latinx, NLW = non-Latinx White; MMSE = Mini Mental State Examination; HAM-D = Hamilton Depression Rating Scale 17-item. All p-values ≥ 0.180.

Table 2
JLO performance and error profile for the full sample.

N = 107	MEAN (ST. DEV.)	MIN	MAX
TOTAL CORRECT ITEMS	21.91 (4.89)	7	30
TOTAL LINES INCORRECT	7.99 (4.809)	0	23
OBLIQUE LINE ERRORS			
z-score	0.0 (1.0)	−1.58	2.58
%	28.09 (17.68)	0	73.68
HV LINE ERRORS			
z-score	0.0 (1.0)	−0.35	7.72
%	2.45 (6.96)	0	56.25
OBLIQUE EFFECT (z-score)	−0.37 (2.50)	−4.51	4.78

NOTE: HV = horizontal + vertical; individual oblique and HV line errors are also presented as percentages for ease interpretation while oblique effect z-scores were multiplied by −1 so that higher z-scores represented higher oblique error production relative to HV line error production.

3.4. Neuroimaging and the oblique effect

3.4.1. Connectome metrics

Separate multivariable linear regression models adjusting for sex, education, and MMSE did not reveal any significant associations between zOE and global system properties of clustering coefficient (β = −0.13, t(100) = -1.43, p = 0.154), path length (β = 0.17, t(100) = 1.83, p = 0.069), or network efficiency (β = −0.11, t(100) = -1.15, p = 0.253).

3.4.2. Hierarchical modularity analyses

After correcting for multiple comparisons, results examining the differences in modular organization between the median-split zOblique groups adjusting for sex, education, and MMSE revealed a differential pattern of affiliation in the left hemisphere involving the caudal middle frontal gyrus (average V: high zOblique error group = 0.13 ± 0.13, low zOblique error group = 0.22 ± 0.16, FDR corrected p = 0.003, nodal-level corrected p = 0.001) and the right hemisphere involving the precuneus (average V: high zOblique error group = 0.09 ± 0.07, low zOblique error group = 0.16 ± 0.14, FDR corrected p = 0.003, nodal-level corrected p = 0.001) (Fig. 2). For individuals in the high zOblique group, the caudal middle frontal gyrus formed a module by its affiliation with the left lateral and medial orbitofrontal gyrus, left dorsolateral prefrontal region (i.e., pars orbitalis, pars triangularis, and pars opercularis), left rostral and caudal anterior cingulate, and the left middle and superior frontal gyri. Participants in the low zOblique group exhibited a different, much more concise module. Instead of modular affiliation that included much of the prefrontal cortex, they exhibited a modular organization of affiliation between the left caudal middle frontal gyrus and the left lateral orbitofrontal gyrus, as well as the left basal ganglia, i.e., the left thalamus, caudate, and accumbens (Fig. 2a). Additionally, for individuals in the high zOblique group, the right precuneus formed a modular affiliation with the right pericalcarine, right

Table 3
Hierarchical linear regressions for cognitive domains and the oblique effect.

	B	T	P	R^2
EXECUTIVE FUNCTIONING (EF)				.28
SEX**	.33	3.64	<.001	
EDUCATION	-.07	0.74	.461	
MMSE	-.07	−0.72	.469	
EF**	-.46	−3.97	<.001	
ATTENTION/INFORMATION PROCESSING (AIP)				.14
SEX**	.25	2.60	.011	
EDUCATION	-.07	−0.74	.459	
MMSE*	-.19	−1.85	.067	
AIP	-.14	−1.31	.191	

Note: *p ≤ 0.05, **p ≤ 0.01; adding a sex-by-EF interaction term to the EF model did not change the reported results.

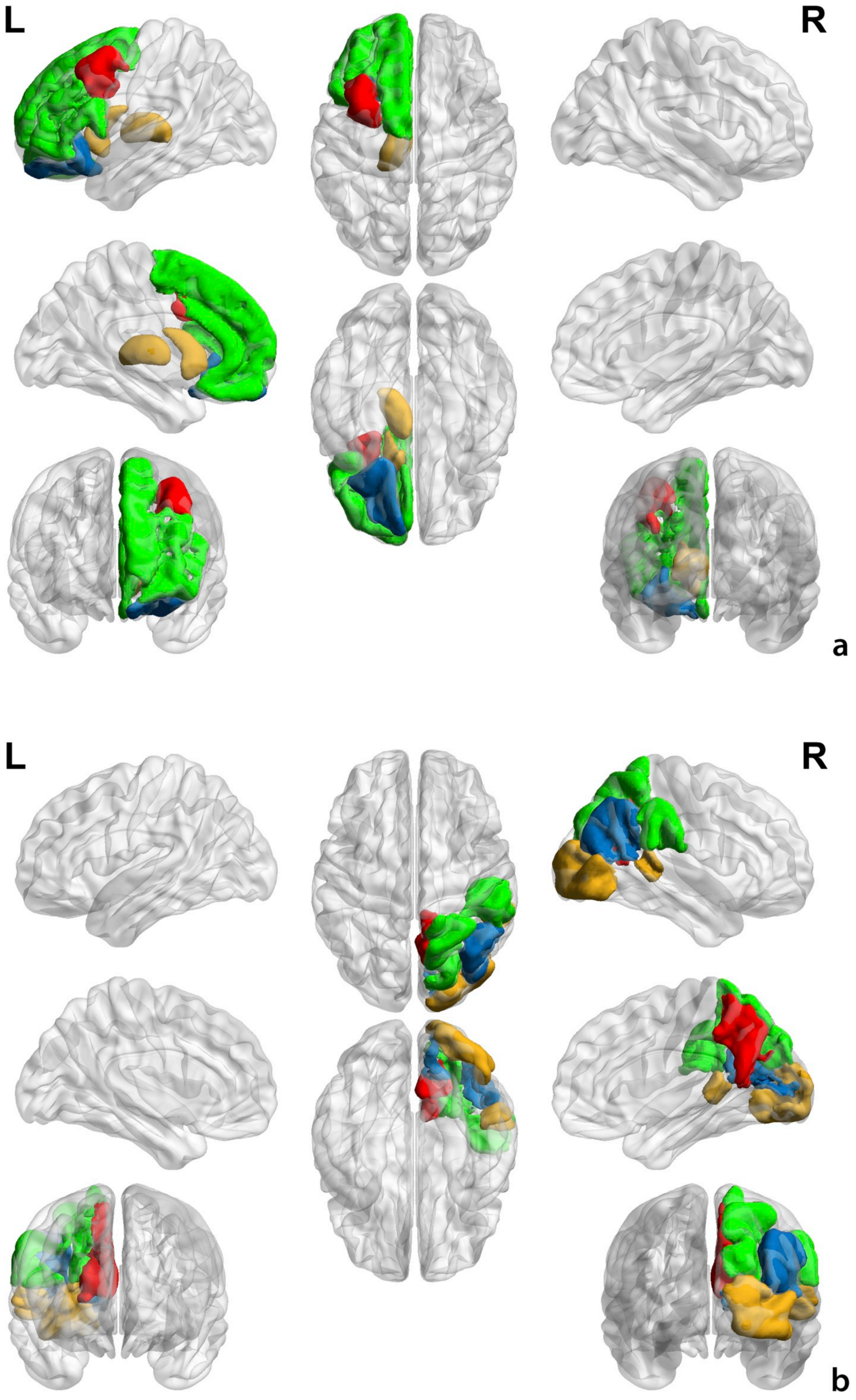

Fig. 2. A representation of the modular organization differences between high versus low zOblique error production based on significantly different V values (shown in red) in the left caudal middle frontal region (2a) and the right precuneus (2b), separately. In 2a, participants in the high oblique error group showed a higher degree of modular integration of the left caudal middle frontal region (in red) with the left lateral orbitofrontal gyrus (in blue), and the left medial orbitofrontal gyrus, pars orbitalis, pars triangularis, pars opercularis, rostral and caudal anterior cingulate, and middle and superior frontal gyri (in green). In contrast, participants in the low oblique error group showed a higher degree of modular integration of the left caudal middle frontal (in red) with the left lateral orbitofrontal gyrus (in blue) and the left thalamus, caudate, and accumbens (in orange). In 2b, participants in the high oblique error group showed a higher degree of modular integration of the right precuneus (in red) with the right inferior parietal and pericalcarine gyri (in blue), and the right superior parietal and supramarginal gyri (in green). In contrast, participants in the low oblique error group showed a higher degree of modular integration of the right precuneus (in red) with the right inferior parietal and pericalcarine gyri (in blue), and the right lateral occipital gyrus (in orange). (For interpretation of the references to colour in this figure legend, the reader is referred to the Web version of this article.)

inferior and superior parietal and right supramarginal gyri. In contrast, instead of modular affiliation that included superior parietal and supramarginal gyri, participants in the low zOblique group exhibited a modular organization of affiliation between the right precuneus, the right pericalcarine and inferior parietal gyri and the right lateral occipital gyrus (Fig. 2b).

Similar analyses employing the median-split zHV groups (only 24 participants committed HV errors, thus, the median split reflected any HV errors versus no HV errors) revealed a differential pattern of affiliation in the right hemisphere only, it involved the rostral anterior cingulate (average V: any zHV errors = 0.15 ± 0.13, no zHV errors = 0.07 ± 0.08, FDR corrected $p = 0.0004$, nodal-level corrected $p = 0.0003$). For individuals with any zHV errors, the right rostral anterior cingulate formed a module by its affiliation with the right medial and lateral OFC, the right rostral middle frontal gyrus, and the right caudate. Participants with no zHV errors exhibited a different, broader based module. In addition to the right rostral anterior cingulate modular affiliation with the right medial and lateral orbitofrontal gyrus, and the right rostral middle frontal gyrus, the modular organization of affiliation for individuals with no zHV errors also included the right caudal ACC as well as the posterior cingulate, right pars orbitalis and triangularis as well as the right superior frontal and left lateral orbitofrontal gyri. Interestingly, a branch of modular affiliation within extrastriate cortex was only seen in individuals with no zHV errors, however, this result was not significant after FDR correction.

4. Discussion

This study examined the relationships between the oblique effect error profile, as measured by the Judgment of Line Orientation test, cognitive functioning, and brain connectomics in over 100 non-demented, non-depressed older adults. Consistent with prior animal and human literature examining the same visuospatial phenomenon, our participants exhibited the oblique effect, i.e., they made more oblique errors than horizontal and vertical line errors. In addition, the results of this study revealed that lower executive functioning was associated with higher oblique line errors relative to HV errors after adjusting for sex, education, and MMSE. Differences in oblique versus HV error profiles were also noted in structural brain connectivity. More specifically, participants with higher levels of oblique errors differed from participants with lower levels of oblique errors in the modular organization associated with their left frontal lobe and right precuneus while participants with higher levels of HV errors differed from participants with no HV errors in the modular organization associated with their right anterior cingulate. Taken together, results suggest that the oblique effect not only exists in older adults, but that poorer performance on a specific cognitive domain (i.e., executive functioning) is associated with a larger oblique effect and oblique versus HV error profiles differentially associate with alterations of underlying regional modular brain networks in these same individuals.

Results of this study contribute to the literature on the oblique effect and visuospatial processing in older adults in several ways. First, while we deliberately chose cognitive domains that have been previously associated with visuospatial processing (Freeman et al., 2000), only alterations of higher-level executive functioning related to zOE. This association may be due, in part, to the fact that executive skills (including mental rotation and sustained mental set) are critical to errorless JLO performance. Thus, not only does our study provide additional evidence for the relationship between executive functioning and visuospatial abilities, it extends this relationship to executive functioning and the oblique effect on the JLO.

Second, distinctions in the modular organization of the brain networks associated with oblique as well as HV error profiles point toward additional forms of executive functioning that may be differentially required to judge oblique, horizontal and vertical lines. In addition to computations and visual integrations of the magnitudes for both angle and distance reflected in the right hemisphere network associates between the precuneus, inferior parietal, and pericalcarine regions regardless of oblique error group, JLO judgments may also rely on external and internal "compass" cues as well as trial-and-error learning and divergent thinking. For example, external cues that are anchored to the environment or the participant's personal space may aide in accurately judging horizontal lines (level with one's shoulders) and vertical lines (aligned with one's mid-sagittal plane); however, oblique lines may require more internally-derived computations. Thus, participants making more oblique errors may not have effectively disengaged from using external or self-referential cues to facilitate their performance. More specifically, the basal ganglia, uniquely associated with the modular structure of participants in the low oblique error group, is often described as a gating mechanism (Frank, Loughry, & O'Rielly, 2001). Not only does it allow for selective neuronal functions to occur including intracellular maintenance within prefrontal regions important for trial-and-error learning (Frank et al., 2001), the basal ganglia may also help to regulate the functions of the middle frontal versus the lateral orbitofrontal cortex – regions associated with JLO performance during oblique line judgments, regardless of oblique error group. Thus, in the modular organization of the low oblique error group, the basal ganglia may facilitate the network balance between the middle frontal gyrus and its role in spatial as well as executive processing (du Boisgueheneuc et al., 2006), and the lateral orbitofrontal cortex, a region associated with externally-driven executive functions (Gusnard et al., 2001), i.e., activities anchored to the environmental and/or personal space. In contrast, in the modular organization of the high oblique error group, these same prefrontal regions combined not with the basal ganglia, but with an expansive left frontal modular network of competing regions differentially influenced by self-referential tasks (du Boisgueheneuc et al., 2006) that may result in a misappropriation of executive skills and greater oblique errors. When combined with the modular organization of the right precuneus, a network structure that favored affiliation with parieto-occipital regions involved in visuospatial integration during non-self-referential tasks and creative or divergent thinking (Chen et al., 2015) in the low oblique error group, but superior parietal and supramarginal regions associated with egocentric neural encoding (Hebscher et al., 2018) in the high oblique error group, results point toward distinctions in the brain regions and associated cognitive processes at work in the face of low versus high oblique line error production. Lastly, it should be noted that participants with no HV errors showed a lower affiliation between attentional allocation of the anterior cingulate and many of these same prefrontal regions when compared to participants making HV errors further supporting their misappropriated role in oblique line judgments.

While it may seem contradictory that some of our neuroimaging results of a visuospatial task like the JLO included the left hemisphere as opposed to being confined strictly to the right hemisphere as previously documented (Benton et al., 1975; Ng et al., 2000; Trahan, 1998), there is support for left hemispheric involvement in the literature. For example, a study of patients with non-fluent agrammatic primary progressive aphasia reported that these patients demonstrated impairment in performing visuospatial tasks, and that this impairment was associated with degradation of white matter pathways in the left inferior frontal lobe (Watson et al., 2018). In addition, Kim et al. (1984) reported that patients with lesions of the left frontal lobe were often impaired in visuospatial functions (Kim et al., 1984). The fact that these studies described degradation in left frontal neuroanatomy associated with visuospatial impairment is consistent with our results reporting the differential pattern of affiliation confined to the left frontal lobe for individuals with higher compared to lower oblique error production. Additionally, the JLO task requirement for verbalization in responding may also contribute to the left hemisphere involvement independent of oblique error group (Geffen et al., 1971). Regardless of verbal codability, several investigators have postulated that visuospatial tasks that are more complex in nature – as we would argue judging oblique line placement is – may be carried out more efficiently by the analytic ability of the left hemisphere (Berlucchi et al., 1979; De Renzi, Faglioni and Scotti, 1971; Umilta et al., 1974). This is further supported by the fact that success versus failure in judging HV line placement – a less complex line judgment than an oblique line evaluation – was confined to a right hemisphere modular network. Thus, our results extend the evidence for left hemisphere involvement in visuospatial task performance to otherwise healthy older adults judging more complex oblique lines compared to more straightforward HV lines.

Consistent with initial work investigating the relationship between age and JLO errors (Benton et al., 1975), older age was not associated with the oblique effect error profile in our sample. However, women produced more oblique errors relative to HV errors than men in our study. Although we controlled for sex in our analyses, sex differences in the oblique effect may bolster our argument for the inclusion of the left hemisphere modular structure described above. From a clinical standpoint, sex-differences in the oblique effect may point toward important cognitive evaluation considerations. While impaired visuospatial processing may be an early indicator of cognitive decline (McKhann et al., 1984) and pathological aging (Freeman et al., 2000), most cognitive evaluations for dementia rely heavily on tests of *verbal* learning and memory – areas where women out-perform men (Aartsen et al., 2004; Herlitz et al., 1999; Lewin et al., 2001). As a result, women may be at a distinct disadvantage for appropriate diagnoses of cognitive impairment or dementia (Sundermann et al., 2016). Incorporating tasks into neuropsychological evaluations that rely on spatial and/or perceptual functioning, including identification of the oblique effect, where men out-perform women (Voyer et al., 1995), may improve early detection and diagnosis of dementia in women.

Although this study has potentially important empirical and clinical implications, it is not without its limitations. Due to the cross-sectional nature of our investigation, we cannot determine causality in the associations between executive functioning, disparities in the modular organization of the structural networks, and the oblique effect observed. Furthermore, we did not reveal any significant graph theory associates to the oblique effect error profile despite one trend. This may be due, in part, to the fact that our zOE metric included the entire spectrum of behaviors ranging from more oblique than HV errors to no errors at all, or that only 24 participants produced HV errors. Including a broader range of older adults, particularly those at risk for dementia with known brain structure vulnerabilities that may produce more JLO errors generally including more HV errors, or a younger control group may provide the additional variation needed to reveal significant associates to these in-depth integrative patterns of brain connectomics.

Strengths of this study include the use of tract-based structural connectomics to begin to understand the interplay between T1-weighted gray matter regions (cortical and subcortical) and their connecting DTI-derived white matter tracts as it relates to the oblique effect in older adults. Furthermore, we utilized probabilistic tractography to allow for better delineation of crossing fibers in the brain, and ultimately a more accurate depiction of white matter tracts in regions with dense fiber connections (Zhan et al., 2015). Lastly, we were able to adjust for important confounds in our analyses, including our PLACE analyses, to increase the accuracy of our associations.

In conclusion, this study presents evidence for the oblique effect in older adults including cognitive correlates and modular brain network differences associated with oblique versus HV line errors in these same older adults. Future longitudinal work should examine how changes in brain structure may influence performance on visuospatial tasks that measure the oblique effect error profile and whether these structural alterations are more pronounced in women and/or individuals at risk for dementia. These longitudinal studies are essential to validate and further understand the utility of the oblique effect error profile as a potential early cognitive, more specifically, visuospatial, marker of neurodegenerative disease.

CRediT authorship contribution statement

Jamie C. Peven: Data curation, Formal analysis, Investigation, Methodology, Project administration, Validation, Writing - original draft. **Yurong Chen:** Formal analysis, Software, Validation, Visualization. **Lei Guo:** Formal analysis, Software, Validation, Visualization. **Liang Zhan:** Formal analysis, Software, Supervision, Validation, Visualization. **Elizabeth A. Boots:** Data curation, Investigation, Project administration, Validation. **Catherine Dion:** Data curation. **David J. Libon:** Validation, Writing - review & editing. **Kenneth M. Heilman:** Conceptualization, Validation, Writing - review & editing. **Melissa Lamar:** Conceptualization, Formal analysis, Funding acquisition, Investigation, Methodology, Project administration, Software, Supervision, Validation, Writing - original draft.

Acknowledgements

The authors would like to thank the participants and staff of this study. The authors would also like to thank the study staff for their contribution to the development of this project. This work was supported by the National Institutes of Health, National Institute on Aging, United States: K01 AG040192 and R21 AG048176. Additionally, aspects of this project were supported by the National Center for Research Resources, National Institutes of Health, United States: 1S10RR028898.

Appendix A. Supplementary data

Supplementary data to this article can be found online at https://doi.org/10.1016/j.neuropsychologia.2019.107236.

Conflict of interest/disclosure statement

The authors have no conflict of interest to report.

References

Mori, S., Crain, B., Chacko, V., van Zijl, P., 1999. Three-dimensional tracking of axonal projections in the brain by magnetic resonance imaging. Ann. Neurol. 45, 2–3. https://doi.org/10.1002/1531-8249(199902)45:2<265::AID-ANA21>3.0.CO, 265-269.

Aartsen, M., Martin, M., Zimprich, D., 2004. Gender differences in level and change in cognitive functioning. Gerontology 50 (1), 35–38.

Ajilore, O., Lamar, M., Leow, A., Zhang, A., Yang, S., Kumar, A., 2014. Graph theory analysis of cortical-subcortical networks in late-life depression. Am. J. Geriatr. Psychiatry 22 (2), 195–206.

Appelle, S., 1972. Perception and discrimination as a function of stimulus orientation: the "oblique effect" in man and animals. Psychol. Bull. 78 (4), 266–278.

Arakawa, K., Tobimatsu, S., Kurita-Tashima, S., Nakayama, M., Kira, J., Kato, M., 2000. Effects of stimulus orientation on spatial frequency function of the visual evoked potential. Exp. Brain Res. 131 (1), 121–125.

Attneave, F., Olson, R., 1967. Disciminability of stimuli varying in physical and retinal orientation. J. Exp. Psychol. 74 (2), 149–157.

Beck, A., Steer, R., 1990. Manual for the Beck Anxiety Inventory. Psychological Corporation, San Antonio, TX.

Beck, A., Steer, R., Brown, G., 1996. BDI-II: Beck Depression Inventory, vol. 78. Pearson.

Benton, A., Hannay, H., Varney, N., 1975. Visual perception of line direction in patients with unilateral brain disease. Neurology 25 (10), 907–910.

Benton, A., Hamsher, K., Varney, N., Spreen, O., 1983. Judgment of Line Orientation. Oxford University Press, New York, NY.

Berlucchi, G., Brizzolara, D., Marzi, C., Rizzolatti, G., Umilta, C., 1979. The role of stimulus discriminability and verbal codability in hemispheric specialization for visuospatial tasks. Neuropsychologia 17 (2), 195–202.

Bonds, A., 1982. An "oblique effect" in the visual evoked potential of the cat. Exp. Brain Res. 46 (1), 151–154.

Brown, J., Terashima, K., Burggren, A., Ercoli, L., Miller, K., Small, G., Bookheimer, S., 2011. Brain network local interconnectivity loss in aging APOE-4 allele carriers. Proc. Natl. Acad. Sci. 108 (51), 20760–20765.

Cabeza, R., Daselaar, S., Dolcos, F., Prince, S., Budde, M., Nyberg, L., 2004. Task-independent and task-specific age effects on brain activity during working memory, visual attention and episodic retrieval. Cerebr. Cortex 14 (4), 364–375.

Charlton, R., Barrick, T., McIntyre, D., Shen, Y., O'Sullivan, M., Howe, F., Markus, H., 2006. White matter damage on diffusion tensor imaging correlates with age-related cognitive decline. Neurology 66 (2), 217–222.

Charlton, R., Schiavone, F., Barrick, T., Morris, R., Markus, H., 2010. Diffusion tensor imaging detects age related white matter change over a 2 year follow-up which is associated with working memory decline. J. Neurol. Neurosurg. Psychiatry 81 (1), 13–19.

Charlton, R., Lamar, M., Zhang, A., Yang, S., Ajilore, O., Kumar, A., 2014. White-matter tract integrity in late-life depression: associations with severity and cognition. Psychol. Med. 44, 1427–1437.

Chen, Q.L., Xu, T., Yang, W.J., Li, Y.D., Sun, J.Z., Wang, K.C., et al., 2015. Individual differences in verbal creative thinking are reflected in the precuneus. Neuropsychologia 75, 441–449.

Coffey, C., Saxton, J., Ratcliff, G., Bryan, R., Lucke, J., 1999. Relation of education to brain size in normal aging: implications for the reserve hypothesis. Neurology 53 (1). https://doi.org/10.1212/WNL.53.1.189.

Cohen, J., Penney, D., Davis, R., Libon, D., Swenson, R., Ajilore, O., Lamar, M., 2014. Digital clock drawing: differentiating "thinking" versus "doing" in younger and older adults with depression. J. Int. Neuropsychol. Soc. 20 (9), 920–928.

Coppola, D., White, L., Fitzpatrick, D., Purves, D., 1998. Unequal representation of cardinal and oblique contours in ferret visual cortex. Proc. Natl. Acad. Sci. 95 (5), 2621–2623.

Cosgrove, K., Mazure, C., Staley, J., 2007. Evolving knowledge of sex differences in brain structure, function, and chemistry. Biol. Psychiatry 62 (8), 847–855.

De Renzi, E., Faglioni, P., Scotti, G., 1971. Judgment of spatial orientation in patients with focal brain damage. J. Neurol. Neurosurg. Psychiatry 34 (5), 489–495.

De Valois, R., Yund, E., Hepler, N., 1982. The orientation and direction selectivity of cells in the macaque visual cortex. Vis. Res. 22 (5), 531–544.

Desikan, R., Segonne, F., Fischl, B., Quinn, B., Dickerson, B., Blacker, D., Albert, M., 2006. An automated labeling system for subdividing the human cerebral cortex on MRI scans into gyral based regions of interest. Neuroimage 31 (3), 968–980.

Destrieux, C., Fischl, B., Dale, A., Halgren, E., 2010. Automatic parcellation of human cortical gyri and sulci using standard anatomical nomenclature. Neuroimage 53 (1), 1–15.

Dolcos, F., Rice, H., Cabeza, R., 2002. Hemispheric asymmetry and aging: right hemisphere decline or asymmetry reduction. Neurosci. Biobehav. Rev. 26 (7), 819–825.

Dragoi, V., Sharma, J., Sur, M., 2000. Adaptation-induced plasticity of orientation tuning in adult visual cortex. Neuron 28 (1), 287–298.

du Boisgueheneuc, F., Levy, R., Volle, E., Seassau, M., Duffau, H., Kinkingnehun, S., Dubois, B., 2006. Functions of the left superior frontal gyrus in humans: a lesion study. Brain 129 (12), 3315–3328.

Essock, E., 1980. The oblique effect of stimulus identification considered with respect to two classes of oblique effects. Perception 9 (1), 37–46.

Finton, M., Lucas, J., Graff-Radford, N., Uitti, R., 1998. Analysis of visuospatial errors in patients with Alzheimer's disease or Parkinson's disease. J. Clin. Exp. Neuropsychol. 20 (2), 186–193.

Fischl, B., Van Der Kouwe, A., Destrieux, C., Halgren, E., Segonne, F., Salat, D., Caviness, V., 2004. Automatically parcellating the human cerebral cortex. Cerebr. Cortex 14 (1), 11–22.

Folstein, M., Folstein, S., McHugh, P., 1975. Mini-mental state": a practical method for grading the cognitive state of patients for the clinician. J. Psychiatr. Res. 12 (3), 189–198.

Frank, M.J., Loughry, B., O'Rielly, R.C., 2001. Interactions between frontal cortex and basal ganglia in working memory: a computational model. Cognit. Affect Behav. Neurosci. 1 (2), 137–160.

Freeman, R., Giovannetti, T., Lamar, M., Cloud, B., Stern, R., Kaplan, E., Libon, D., 2000. Visuoconstructional problems in dementia: contribution of executive systems functions. Neuropsychology 14 (3).

Furmanski, C., Engel, S., 2000. An oblique effect in human primary visual cortex. Nat. Neurosci. 3 (6), 535–536.

GadElkarim, J., Schonfeld, D., Ajilore, O., Zhan, L., Zhang, A., Feusner, J., Leow, A., 2012. A framework for quantifying node-level community structure group differences in brain connectivity networks. Int. Conf. Med. Image Comput. Comput. Assist. Interv. 15, 196–203.

GadElkarim, J., Ajilore, O., Schonfeld, D., Zhan, L., Thompson, P., Feusner, J., Leow, A., 2014. Investigating brain community structure abnormalities in bipolar disorder using path length associated community estimation. Hum. Brain Mapp. 35 (5), 2253–2264.

Ganguli, M., Snitz, B., Lee, C., Vanderbilt, J., Saxton, J., Chang, C., 2010. Age and education effects and norms on a cognitive test battery from a population-based cohort: the Monongahela-Youghiogheny Healthy Aging Team. Aging Ment. Health 14 (1), 100–107.

Geerligs, L., Rubinov, M., Henson, R., 2015. State and trait components of functional connectivity: individual differences vary with mental state. J. Neurosci. 35 (41), 13949–13961.

Geffen, G., Bradshaw, J., Wallace, G., 1971. Interhemispheric effects on reaction time to verbal and nonverbal visual stimuli. J. Exp. Psychol. 87 (3), 415–422.

Geisler, W., Albrecht, D., 1997. Visual cortex neurons in monkeys and cats: detection, discrimination, and identification. Vis. Neurosci. 14, 897–919.

Gonzales, M., Ajilore, O., Charlton, R., Cohen, J., Yang, S., Sieg, E., Lamar, M., 2017. Divergent influences of cardiovascular disease risk factor domains on cognition, grey, and white matter morphology. Psychosom. Med. 79 (5), 541–548.

Gusnard, D., Akbudak, E., Shulman, G., Raichle, M.E., 2001. Medial prefrontal cortex and self-referential mental activity: relation to a default mode of brain function. Proc. Natl. Acad. Sci. 98 (7), 4259–4264.

Hamilton, M., 1960. A rating scale for depression. J. Neurol. Neurosurg. Psychiatry 23 (1), 56–62.

Hebscher, M., Levine, B., Gilboa, A., 2018. The precuneus and hippocampus contribute to individual differences in the unfolding of spatial representations during episodic autobiographical memory. Neuropsychologia 110, 123–133.

Herlitz, A., Airaksinen, E., Nordstrom, E., 1999. Sex differences in episodic memory: the impact of verbal and visuospatial ability. Neuropsychology 13 (4), 590–597.

Higgins, G., Stultz, K., 1950. Variation of visual acuity with various test-object orientations and viewing conditions. J. Opt. Soc. Am. 40 (3), 135–137.

Kanaan, R., Allin, M., Picchioni, M., Barker, G., Daly, E., Shergill, S., McGuire, P., 2012. Gender differences in white matter microstructure. PLoS One 7 (6), e38272.

Kim, Y., Morrow, L., Passafiume, D., Boller, F., 1984. Visuoperceptual and visuomotor abilities and locus of lesion. Neuropsychologia 22 (2), 177–185.

Lamar, M., Podell, K., Carew, T., Cloud, B., Resh, R., Kennedy, C., Libon, D., 1997. Perseverative behavior in Alzheimer's disease and subcortical ischemic vascular dementia. Neuropsychology 11 (4).

Lamar, M., Rubin, L., Ajilore, O., Charlton, R., Zhang, A., Yang, S., Kumar, A., 2015. What metabolic syndrome contributes to brain outcomes in African American & Caucasian cohorts. Curr. Alzheimer Res. 12 (7), 640–647.

Lamar, M., Ajilore, O., Leow, A., Charlton, R., Cohen, J., GadElkarim, J., Libon, D., 2016. Cognitive and connectome properties detectable through individual differences in graphomotor organization. Neuropsychologia 85, 301–309.

Leehey, S., Moskowitz-Cook, A., Brill, S., Heid, R., 1975. Orientational anisotropy in infant vision. Science 190 (4217), 900–902.

Lewin, C., Wolgers, G., Herlitz, A., 2001. Sex differences favoring women in verbal but not in visuospatial episodic memory. Neuropsychology 15 (2).

Li, B., Peterson, M., Freeman, R., 2003. Oblique effect: a neural basis in the visual cortex. J. Neurophysiol. 90 (1), 204–217.

Maffei, L., Campbell, F., 1970. Neurophysiological Localization of the Vertical and Horizontal Visual Coordinates in Man, vol. 167, pp. 386–387, 3917.

Mansfield, R., 1974. Neural basis of orientation perception in primate vision. Science 186 (4169), 1133–1135.

McKhann, G., Drachman, D., Folstein, M., Katzman, R., Price, D., Stadlan, E., 1984. Clinical diagnosis of Alzheimer's disease report of the NINCDS-ADRDA work group* under the auspices of department of Health and human services task force on Alzheimer's disease. Neurology 34 (7).

McMahon, M., Macleod, D., 2003. The origin of the oblique effect examined with pattern adaptation and masking. J. Vis. 3 (3), 4-4.

Mehta, Z., Newcome, F., 1991. A role for the left hemisphere in spatial processing. Cortex 27 (2), 153–157.

Ng, V., Eslinger, P., Williams, S., Brammer, M., Bullmore, E., Andrew, C., Benton, A., 2000. Hemispheric preference in visuospatial processing: a complementary approach with fMRI and lesion studies. Hum. Brain Mapp. 10 (2), 80–86.

Orban, G., Vandenbussche, E., Vogels, R., 1984. Human orientation discrimination tested with long stimuli. Vis. Res. 24 (2), 121–128.

Reitan, R., Wolfson, D., 1985. The Halstead-Reitan neuropsychological test battery: theory and clinical interpretation. In: Reitan Neuropsychology, vol. 4.

Rey, G.J., Feldman, E., Rivas-Vazquez, R., Levin, B.E., Benton, A., 1999. Neuropsychological test development and normative data on Hispanics. Arch. Clin. Neuropsychol. 14 (7), 593–601.

Rubinov, M., Sporns, O., 2010. Complex network measures of brain connectivity: uses and interpretations. Neuroimage 52 (3), 1059–1069.

Rubinov, M., Sporns, O., 2011. Weight-conserving characterization of complex functional brain networks. Neuroimage 56 (4), 2068–2079.

Ska, B., Poissant, A., Joanette, Y., 1990. Line orientation judgment in normal elderly and subjects with dementia of Alzheimer's type. J. Clin. Exp. Neuropsychol. 12 (5), 695–702.

Sokol, S., Moskowitz, A., Hansen, V., 1987. Electrophysiological evidence for the oblique effect in human infants. Investig. Ophthalmol. Vis. Sci. 28 (4), 731–735.

Spitzer, R.L., Williams, J.B., Gibbon, M., First, M.B., 1992. The structured clinical Interview for DSM-III-R (SCID) I: history, rationale, and description. Arch. Gen. Psychiatr. 49 (8), 624–629.

Sundermann, E., Maki, P., Rubin, L., Lipton, R., Landau, S., Biegon, A., Jagust, W., 2016. Female advantage in verbal memory: evidence of sex-specific cognitive reserve. Neurology 87, 1916–1924.

Trahan, D., 1998. Judgment of line orientation in patients with unilateral cerebrovascular lesions. Assessment 5 (3), 227–235.

Tunc, B., Solmaz, B., Parker, D., Satterthwaite, T., Elliott, M., Calkins, M., Verma, R., 2016. Establishing a link between sex-related differences in structural connectome and behavior. Philos. Trans. R. Soc. Lond. B Biol. Sci. 371 (1688).

Umilta, C., Rizzolatti, G., Marzi, C., Zamboni, G., Franzini, C., Camarda, R., Berlucchi, G., 1974. Hemispheric differences in the discrimination of line orientation. Neuropsychologia 12 (2), 165–174.

Voyer, D., Voyer, S., Bryden, M., 1995. Magnitude of sex differences in spatial abilities: a meta-analysis and consideration of critical variables. Psychol. Bull. 117 (2).

Watson, C., Possin, K., Allen, I., Hubbard, H., Meyer, M., Welch, A., Gorno-Tempini, M., 2018. Visuospatial functioning in the primary progressive aphasias. J. Int. Neuropsychol. Soc. 24 (3), 259–268. https://doi.org/10.1017/S1355617717000984.

Wechsler, D., 1997. WAIS-III: Wechsler Adult Intelligence Scale. Psychological Corporation, San Antonio, TX.

Wechsler, D., 2014. Wechsler Adult Intelligence Scale - Fourth Edition (WAIS-IV). Psychological Corporation, San Antonio, TX.

Wen, W., Zhu, W., He, Y., Kochan, N., Reppermund, S., Slavin, M., Sachdev, P., 2011. Discrete neuroanatomical networks are associated with specific cognitive abilities in old age. J. Neurosci. 31 (4), 1204–1212.

Westheimer, G., 2003. Meridional anisotropy in visual processing: implications for the neural site of the oblique effect. Vis. Res. 43 (22), 2281–2289.

Xia, M., Wang, J., He, Y., 2013. BrainNet Viewer: a network visualization tool for human brain connectomics. PLoS One 8 (7), e68910.

Ye, A., Zhan, L., Conrin, S., GadElkarim, J., Zhang, A., Yang, S., Leow, A., 2015. Measuring embeddedness: hierarchical scale-dependent information exchange efficiency of the human brain connectome. Hum. Brain Mapp. 36 (9), 3653–3665.

Zhan, L., Zhou, J., Wang, Y., Jin, Y., Jahanshad, N., Prasad, G., Initiative, A.s.D.N., 2015. Comparison of nine tractography algorithms for detecting abnormal structural brain networks in Alzheimer's disease. Front. Aging Neurosci. 7.